Author Manuscript

Author Manuscript

Author Manuscript

Author Manuscript

Enhanced morphological transformation of human lung epithelial cells by continuous exposure to cellulose nanocrystals

E.R. Kisin[a,1], **N. Yanamala**[a,1], **D. Rodin**[b], **A. Menas**[a], **M. Farcas**[a], **M. Russo**[a,c], **S. Guppi**[a], **T.O. Khaliullin**[a,d], **I. Iavicoli**[e], **M. Harper**[f], **A. Star**[g], **V.E. Kagan**[h,i,j], **A.A. Shvedova**[a,d,*]

[a]EAB, HELD, NIOSH, CDC, Morgantown, WV, USA

[b]Institute for Personalized and Translational Medicine, Ariel University, Ariel, Israel

[c]Institute of Public Health, Section of Occupational Medicine, Catholic University of the Sacred Heart, Rome, Italy

[d]Department of Physiology & Pharmacology, WVU, Morgantown, WV, USA

[e]Department of Public Health, University of Naples Federico II, Naples, Italy

[f]Zefon International, Ocala, FL, USA

[g]Department of Chemistry, University of Pittsburgh, Pittsburgh, PA, USA

[h]Department of Environmental & Occupational Health, University of Pittsburgh, Pittsburgh, PA, USA

[i]Center for Free Radical and Antioxidant Health, University of Pittsburgh, Pittsburgh, PA, USA

[j]Laboratory of Navigational Redox Lipidomics, IM Sechenov Moscow State Medical University, Moscow, Russian Federation

Abstract

Cellulose nanocrystals (CNC), also known as nanowhiskers, have recently gained much attention due to their biodegradable nature, advantageous chemical and mechanical properties, economic value and renewability thus making them attractive for a wide range of applications. However,

[*]Corresponding author. Exposure Assessment Branch (MS-2015), 1095 Willowdale Road, Morgantown, WV, 26505, USA. ats1@cdc.gov (A.A. Shvedova).
[1]Both authors' contributed equally to the manuscript.

Disclaimer

before these materials can be considered for potential uses, investigation of their toxicity is prudent. Although CNC exposures are associated with pulmonary inflammation and damage as well as oxidative stress responses and genotoxicity *in vivo*, studies evaluating cell transformation or tumorigenic potential of CNC's were not previously conducted. In this study, we aimed to assess the neoplastic-like transformation potential of two forms of CNC derived from wood (powder and gel) in human pulmonary epithelial cells (BEAS-2B) in comparison to fibrous tremolite (TF), known to induce lung cancer. Short-term exposure to CNC or TF induced intracellular ROS increase and DNA damage while long-term exposure resulted in neoplastic-like transformation demonstrated by increased cell proliferation, anchorage-independent growth, migration and invasion. The increased proliferative responses were also in-agreement with observed levels of pro-inflammatory cytokines. Based on the hierarchical clustering analysis (HCA) of the inflammatory cytokine responses, CNC powder was segregated from the control and CNC-gel samples. This suggests that CNC may have the ability to influence neoplastic-like transformation events in pulmonary epithelial cells and that such effects are dependent on the type/ form of CNC. Further studies focusing on determining and understanding molecular mechanisms underlying potential CNC cell transformation events and their likelihood to induce tumorigenic effects *in vivo* are highly warranted.

Keywords

1. Introduction

Nanocellulose (NC) is a highly versatile material with unique properties that allow its use in numerous industrial applications. Derived from a diversity of sources of cellulosic biomass, including those from the forest, agricultural and recycling industries as well as bacteria and tunicates (Shatkin and Kim, 2015), NC is unique in that it is bio-based, renewable, biodegradable, and relatively inexpensive (Roman, 2015). Currently NC is available on market in different forms that can be modified for use in a wide range of applications including oil and gas industries, adhesives, paints and coatings, nonwoven materials, composites, food, cosmetics, pharmaceuticals and many other materials (Österberg and Cranston, 2014; Stefaniak et al., 2014). NC has been widely tested by many companies, but only a few commercial applications have been reported to date. Among them are use of NC in cosmetics (DeLeon Cosmetics), gel inks as a thickener (Mitsubishi Pencil Co Ltd and DKS Co Ltd), and for the production of adult diapers (Nippon Paper Crecia Co., Ltd.). Additionally, cellulose could be used as an asbestos substitute for asbestos cement products (Park, 2018). Despite many technological challenges, NC production and application is growing, which could lead to a rapid increase in people exposed to this nanomaterial. Indeed, it was estimated that nanocellulose could increase the U.S. economy by $600 billion by 2020 (https://technology.risiinfo.com/mills/north-america/risi-nanocellulose-study-transformational-new-material-forest-products-industry). Emerging technologies often develop before appropriate knowledge of the risks to workers, consumers/users have been obtained, and NC is no exception (Howard and Murashov, 2009).

One of the major forms of NC, crystalline nanocellulose (CNC), is extremely strong and has unique electrical and optical properties. CNC also carry a charge and is chemically active. However, some properties of CNC, such as high aspect ratio and stiffness, could raise concern of adverse human health effects (Chen et al., 2012). Currently, the number of published studies on CNC toxicity is limited with most of these reports investigating short-term rather than longer-term exposures. For instance, *in vivo* studies reported pulmonary inflammation and damage, elevated collagen deposition and TGF-β levels as well as oxidative stress responses, genotoxicity and long-term pulmonary retention (Catalan et al., 2017; Park et al., 2018; Shatkin and Kim, 2015; Shvedova et al., 2016; Yanamala et al., 2014; Joseph et al., 2017; Cullen et al., 2000). Additionally, it was shown that CNC affects innate immunity and has adjuvant effects in OVA-mouse model (Park et al., 2018; Wang et al., 2019). Moreover, a number of *in vitro* studies reported cytotoxic responses accompanied by increase in release of inflammatory mediators, particle cellular uptake, oxidative stress and proliferation in response to CNC exposure (Catalan et al., 2015; Menas et al., 2017; Wang et al., 2019; Yanamala et al., 2016; Endes et al., 2014). Although the research progress has been made to understand the CNC-induced toxicity, as noted by referred studies, yet the knowledge gap still exists in term of long-term toxicity effects. This is particularly important since chronic low dose exposure studies that represent realistic workplace conditions are considered more suitable experimental models for risk assessment than single (bolus) acute exposure studies (Oberdorster, 2010; Ede et al., 2019). To date, no studies have evaluated the tumorigenic potential of CNC long-term exposures *in vitro*.

In vitro screening methods employing human cell lines described previously can provide rapid, robust and high-throughput platform for assessing neoplastic-like transformation in cells (Wang et al., 2014). Thus, the present study was aimed to evaluate the potential neoplastic-like transformation inducing ability of two forms of CNC (powder and gel), derived from wood, in comparison to respirable fibrous tremolite. Tremolite asbestos was shown to induce structural cell damage and accumulation of biomarkers for cancer development (Pugnaloni et al., 2013), chromosomal mutations, micronucleus induction and cell transformation *in vitro* (Athanasiou et al., 1992; Srivastava et al., 2010), mesothelioma in rats (Aierken et al., 2014; Davis et al., 1991), lung cancer and malignant mesothelioma in humans (Schneider et al., 1998; Kohyama et al., 2017; Roggli et al., 2002).

Human pulmonary epithelial cells (BEAS-2B) used in the study, is a noncancerous SV-40 immortalized cell line closest to normal bronchial epithelium (Ke et al., 1988) and is commonly used as a model for studying pulmonary carcinogenesis and toxicity (Klein-Szanto et al., 1992; Park et al., 2015; van Agen et al., 1997). Cells undergoing neoplastic transformation usually display hallmarks such as altered morphology, increased proliferation, enhanced cancer cell behavior and *in vivo* tumor formation (Creton et al., 2012; Hanahan and Weinberg, 2011; Wang et al., 2014). Here, by employing cancer cell hallmark assays, we showed that continuous exposure of BEAS-2B cells to occupationally relevant non-toxic concentrations of CNC for 4 weeks caused proliferation, transformation and enhanced invasion/migration. Moreover, inflammatory response induced by CNC powder was segregated from the control and CNC gel-exposed groups. In addition, CNC exposure triggered oxidative stress and DNA damage. Overall, our results show that sub-

chronic exposure to CNC may initiate neoplastic-like transformation *in vitro*. Further studies will assess and validate the tumorigenic potential of CNC under *in vivo* conditions.

2. Materials and methods

2.1. Particle preparation and characterization

CNC in two different forms, powder and gel (10% wt.), were obtained from the USDA Forest Products Laboratory (Madison, WI). Stock solutions of each particle were prepared in United States Pharmacopea (USP) grade water and sterilized by autoclaving followed by brief sonication (30 s) with a probe sonicator (Branson Sonifer 450,10 W continuous output). These stock solutions were further diluted with medium for BEAS-2B cells to prepare chosen test concentrations. Atomic force microscopy (AFM) and dynamic light scattering (DLS) analysis were performed to characterize CNC materials. The AFM and DLS analysis of the CNC samples used in this study were published previously (Shvedova et al., 2016). Respirable tremolite asbestos (Lone Pine, CA (Harper et al., 2014);) was processed by grinding to produce a homogenous material of reduced particle size and characterized by RTI Laboratories using transmission electron microscopy (TEM) to determine fiber length and width and resulting percent of fibers with length 5 and aspect ratio 3. A minimum of 800 particles were counted for accurate characterization.

2.2. Cell culture and long-term exposure to CNC or TF

Noncancerous human bronchial epithelial cells (Ad12-SV40 immortalized) BEAS-2B (ATCC, Manassas, VA) were grown and maintained in Dulbecco's Modified Eagle Medium (DMEM) supplemented with 2 mM glutamine, 5% heat-inactivated fetal bovine serum (FBS) with 1% pen-strep (Invitrogen, Carlsbad, CA). Cells were maintained at 37 °C in a humidified 5% CO_2 incubator during and following exposures. Cells were subjected to four cycles of treatment, 72 h each, with non-toxic concentration of CNC (powder or gel) or respirable TF in three biological replicates. In brief, cells were exposed to 30 $\mu g/cm^2$ of each CNC or 2.5 $\mu g/cm^2$ of TF for 72 h in clear DMEM with 1% FBS. Then, cells were washed twice with PBS, counted and transferred to a new flask to grow in full medium containing 5% FBS for additional 4 days. Afterwards, the same CNC or TF treatment was repeated for another 3 times. At the end of each cycle, a maximum confluence of ~80% was maintained and observed. Cells were counted at the end of each cycle and transferred by 1:4 passages. The unexposed control cells were treated using sterile USP grade water. The relevant concentration of CNC used for exposing cells was chosen based on our previous studies (Menas et al., 2017; Yanamala et al., 2016). Concentration of TF was chosen based on our and other's experiences (Nygren et al., 2004; Athanasiou et al., 1992). The dose investigated in this study (2.5 $\mu g/cm^2$) was the least cytotoxic dose from the separate viability experiments (Fig. S1). Additionally, previous experiments with various asbestos fibers revealed that the concentration of 2.5 $\mu g/cm^2$ had a transformation potential without excessive cytotoxicity (Bocchetta et al., 2000; Qi et al., 2013), but still induced the DNA damage (Ollikainen et al., 1999; Nygren et al., 2004).

2.3. Cell cytotoxicity, intracellular ROS generation and DNA damage

First, we evaluated cell cytotoxicity, intracellular reactive oxygen species (ROS) production and DNA damage induced by exposure to CNC, powder or gel, and TF for 72 h. Cytotoxicity was assessed by measuring cell viability and damage. For viability evaluation, cells were collected by trypsinization, stained with trypan blue and counted using Countess™ FL II automated cell counter (Invitrogen, Grand Island, NY). Cell damage was determined by measuring the level of lactate dehydrogenase (LDH) in cell supernatants. LDH was assayed spectrophotometrically using a Synergy H1 Hybrid Reader (BioTek, Winooski, VT). The reduction of nicotinamide adenine dinucleotide in the presence of lactate to pyruvate using a Lactate Dehydrogenase Reagent Set (Pointe Scientific, Lincoln Park, MI) was monitored at 340 nm. All results are presented as the percent of control, as an average from three independent experiments.

To determine ROS generation induced by CNC or tremolite, cells (1×10^4) per well were placed in a clear bottom black 96 well plates and exposed for 72 h. Following exposure, cells were stained with Hoechst 33,342 (2 μM, Sigma-Aldrich, St. Louis, MO) and 2,7-dichloro-fluorescin diacetate (DCF-DA, 25 μM, Life Technologies, Waltham, MA), a fluorogenic dye that may react with several ROS including hydrogen peroxide, hydroxyl radicals and peroxynitrite, for 45 min. Following incubation, cells were washed twice with PBS and fluorescence values of DCF and Hoechst 33,342 were measured using a microplate reader (Synergy H1, BioTek Instruments, Winooski, VT). The excitation/emission wavelengths for DCF and Hoechst 33,342 were 485/530 nm and 350/460 nm, respectively. Integrated intensity of fluorescent signals in each well were calculated. All results are presented as an average from three independent experiments. Hydrogen peroxide was used as a positive control in this assay (data not shown).

The induction of cellular DNA damage following 72 h exposure to CNC or TF was evaluated by the OxiSelect™ Comet assay (Cell Biolabs, San Diego, CA) detecting single or double strand breaks measured at the individual cell level. Cells (0.5×10^6/well) exposed in 6-well plates for 72 h were trypsinized, mixed with low-melting-point agarose, treated with lysis buffer and alkaline solution, electrophoresed under neutral conditions and stained with DNA dye according with manufacturer instruction. For analysis, we imaged at least 3 wells (at least 150 cells) per exposure using automated microscope Evos FL Auto 2 Imaging (Invitrogen, Grand Island, NY). Comet Assay IV Lite software (Insteam, Bury St Edmunds, UK) was used for DNA damage scoring/evaluation as olive tail moment (OTM). All results are presented as an average from three independent experiments.

2.4. Transmission electron microscopy (TEM) imaging of cells exposed to CNC or TF

After long-term exposure (4 weeks), cells were first fixed in 0.5 ml Karnovsky's fixative (2.5% gluteraldehyde, 2.5% paraformaldehyde in 0.1 M Sodium Cacodylic buffer) and then in 2% osmium tetroxide for 1 h. The cells were then dehydrated and embedded in epon, sectioned and stained with Reynold's lead citrate and uranyl acetate. The sections were imaged on a JEOL 1220 transmission electron microscope.

2.5. Cell proliferation assays

To assess cell proliferation/survival following long-term exposure, colony-forming efficiency (CFE) assay was performed using method published previously (Wang et al., 2014). Briefly, cells from each independent exposure replicate were plated at a density of 6 $\times 10^2$/well in 6-well plates in triplicates. Cells were cultured in full medium for 7 days with one medium change on day 4. Further, cells were washed with PBS, fixed in 4% paraformaldehyde, stained with 1% w/v crystal violet, and dried after being rinsed twice with water. Colony counts were visually scored under the microscope. The mean CFE was calculated, where CFE (%) = (average of treatment colonies/average of solvent control colonies x100).

2.6. Cell morphological transformation evaluation

A morphological transformation assay was performed as previously described (Wang et al., 2014). Shortly, exposed cells were seeded at a density of 500/well in 6-well plates in triplicate and grown in full medium for 14 days with a PBS wash and fresh growth medium supplied every 3 days. On day 14, medium was changed to serum-free for 1 week. On day 21, cells were washed with PBS, fixed in 10% formalin and stained with 1% crystal violet to visualize foci. Type III foci were scored from each treatment under an inverted microscope using cell transformation criteria described by (Sasaki et al., 2012). At least three independent assays for each treatment were performed. The results were normalized to the total measured foci per sample.

2.7. Anchorage-independent agar colony formation

Following long-term exposure, cells from all treatment groups were assayed for anchorage-independent cell proliferation using the CytoSelect 96-Well Cell Transformation Assay Kit (Cell Biolabs, Inc., San Diego, CA). Briefly, a 1.2% agar solution was mixed with an equal volume of 2X DMEM/20% FBS at 37 °C and 50 μL of the prewarmed mixture was transferred to each well in order to form the base agar layer. To prepare the cell agar layer, a 75 μl mixture of agar, DMEM and cells (4×10^5 cells/ml) suspensions (1:1:1) were added to each well of a 96-well plate pre-coated with base layer (5×10^3 cells/well). Once the agar solidified, 100 μl of culture medium was added to each well and incubated for 8 days at 37 °C and 5% CO_2. Culture media was changed every 3 days. To measure anchorage-independent growth, agar-layers were dissolved, lysed, mixed with CyQuant and the fluorescence (485/520 nm) was read by Synergy H1 hybrid multi-mode microplate reader (BioTek Instruments, Inc., Winooski, VT). Three independent assays for each treatment were performed. The results are presented as the percent of control.

2.8. Cell migration and invasion assay

Cells, surviving long-term exposure to CNC or TF, were assayed for migration and invasion capacity using CytoSelect cell migration kit (Cell Biolabs, San Diego, CA). This kit utilizes polycarbonate 8 μm pore size membranes that serves as a barrier to discriminate migratory/invasive cells. For cells invasion portion of the kit the upper surface of the insert membrane was coated with a uniform layer of basement membrane matrix solution. Briefly, suspensions of 1.5×10^5 cells/well (duplicate per treatment) in serum free medium were

placed to the each insert, while medium alone containing 10% FBS, as a chemoattractant, in the lower well of the plate. For both migration and invasion assays, cells were incubated for 24 h, non-migratory/invasive cells were carefully removed from inside insert, while migratory/invasive cells on underside of the well insert were stained with crystal violet (10 min @RT). After gently washing the stained inserts several times in a beaker of water, the inserts were air-dried and were transferred to a clean empty well. Following this, 200 μL of extraction solution was added to each well containing the inserts and 100 μL of the sample was used to measure the OD at 560 nm using Synergy H1 hybrid multi-mode microplate reader (BioTek Instruments, Inc., Winooski, VT). All results were presented as an average from three independent experiments.

2.9. TUNEL apoptosis assay

To measure DNA fragmentation (characteristic of late stage apoptosis), we employed TUNEL assay (AAT Bioquest, Inc, Sunnyvale, CA). Briefly, just for apoptosis measurements, last leg of long-term exposure (week 4) was done in 96-well plates. Cells were seeded at a density of 5×10^3 cells/well and exposed (24 h later) to 30 μg/cm^2 of each CNC for 72 h in clear DMEM with 1% FBS. Then, cells were fixed in 4% formaldehyde and incubated with the TUNEL reaction mixture contained fluorescence dye TF3 modified deoxyuridine 5′-triphosphates (TF3-dUTP). Fluorescent intensity was monitored by Synergy H1 hybrid multi-mode microplate reader (BioTek Instruments, Inc., Winooski, VT) at Ex/Em = 550/590 nm. All results were presented as an average from three independent experiments.

2.10. Evaluation of oxidative stress biomarkers

Oxidative damage was evaluated by the presence of hydroxynonenal-histidine (HNE-His) protein adduct, protein carbonyls and reduced glutathione (GSH/protein-SH) level in the cell homogenates following 4-week sub-chronic exposure to CNC, powder or gel. HNE-His adduct, lipid peroxidation end product, was measured by ELISA using an OxiSelect™ HNE-His adduct kit (Cell Biolabs, Inc., San Diego, CA). The quantity of HNE-His adducts in protein samples were determined by comparing its absorbance with that of a known HNE-BSA standard curve. The level of oxidatively modified proteins in cell homogenates, as assessed by measurement of protein carbonyls, was determined using the Biocell PC ELISA kit (Northwest Life Science Specialties). GSH concentration in cell homogenates was determined using ThioGlo™-3, a maleimide reagent, which produces highly fluorescent adducts upon its reaction with SH-groups. Glutathione content was estimated by an immediate fluorescence response registered upon addition of ThioGlo™-3 to the cells homogenate. To measure total protein thiols, a second reading was performed following the addition of SDS and 1-h incubation in the dark. A standard curve was established by addition of GSH (0.04–4.0 μM) to 100 mM phosphate buffer (PBS, pH 7.4) containing 10 μM ThioGlo™-3. The Synergy™ H1 hybrid multi-mode microplate reader (BioTek Instruments, Inc., Winooski, VT) was employed for the assay of fluorescence using excitation at 388 nm and emission at 500 nm. The data obtained were exported and analyzed using Gen 5™ data analysis software (BioTek Instruments, Inc., Winooski, VT). All results were normalized by the total protein in the samples and averaged from three experiments.

2.11. Biomarkers of inflammation

Levels of various cytokines, chemokine and growth factors in the supernatants of the cells exposed to CNC (powder or gel) and TF for 4 weeks were determined using a Bio-Plex system (Bio Rad, Hercules, CA). Human cytokine 27-Plex immunoassay kit was employed. The concentrations were calculated using Bio-Plex Manager 6.1 software (Bio-Rad, Hercules, CA). Data are expressed as pg/total cells number as an average from two to three independent experiments.

2.12. Hierarchical clustering analysis using R

Hierarchical agglomerative (bottom up) clustering analysis using R (R Core Team, 2014) was performed to identify sets of cytokines whose expression levels were correlated among the CNC samples and PBS-exposed controls. All available raw data values, on the entire panel of cancer biomarkers and inflammatory cytokines, were converted to fold-change and then $\log_2$-transformed prior to the clustering analysis. The clustering results are displayed as a heatmap in which correlated cytokines group together so that those with relatively higher levels appear in graded shades of red and those with lower levels in shades of blue. The heatmap was generated with the package 'heatmap' built for R version 3.1.3, using "Euclidean" distance similarity between the different samples and by employing ward.D2 linkage distance between the members of the clusters.

2.13. Protein assay

Measurements of protein in cell homogenates were performed using a Bio-Rad protein assay kit (Richmond, CA). This is a colorimetric assay for measuring total protein concentration using standard procedure based on the Bradford dye-binding method (Bradford, 1976) by employing the Synergy™ H1 hybrid multi-mode microplate reader (BioTek Instruments, Inc., Winooski, VT).

2.14. Statistical analysis

Statistical analysis was performed using SigmaPlot 14.0 (San Jose, CA). Treatment related differences were compared by one-way ANOVA using all pairwise multiple comparison procedures (Holm-Sidak method). All data are presented as means plus the standard error of the mean (SEM). P values of less than 0.05 were considered a statistically significant.

3. Results

3.1. CNC characterization

According to AFM analysis, CNC particles had average length of 158 ± 97 nm and 209 ± 136 nm and average width of 54 ± 17 nm and 37 ± 15 nm for CNC powder and gel, respectively (Table S1). Hydrodynamic diameters were measured by DLS as 149.8 ± 2.6 nm for CNC powder and 137.5 ± 1.2 nm for gel, in good agreement with AFM findings (Shvedova et al., 2016). Overall AFM and DLS analysis revealed that CNC powder exhibited slightly larger widths and hydrodynamic diameters compared to CNC gel, suggesting differences in their particle characteristics and size distributions (Table S1). Mean length and width of the tremolite fibers - as estimated by TEM analysis - is presented

in Table S1 (6.56 ± 0.21 μm and 0.31 ± 0.01 μm, respectively) with an aspect ratio of 25.73 ± 0.92. The percentage of fibers with length 5 μm and aspect ratio 3 was estimated as 45.9%.

3.2. Cell cytotoxicity, intracellular ROS and DNA damage

Cytotoxicity, intracellular ROS production and DNA damage were evaluated following 72 h exposure to CNC, powder or gel, and TF. No viability changes were found after exposure to either CNC or TF as compared to control (Fig. S1B). Significant elevation in the level of LDH (by 33%) was found only after exposure to TF (Fig. S2A). On the other hand, all tested materials elicited significant increase in intracellular ROS species (average 8.5-fold of control, Fig. S2B). OTM was used for DNA damage evaluation in the cells exposed to CNC and TF for 72 h. All three tested materials significantly increased DNA damage (average 1.64-fold) in comparison to control (Fig. S2C).

3.3. Cell morphology, proliferation and transformation

TEM was employed to assess morphological/phenotypic changes in cells after long-term exposure to CNC or respirable TF materials (Fig. 1). Control BEAS-2B cells (Fig. 1A) showed their typical ultra-structural features with well-preserved cytoplasm, indented nucleus, with a number of intact organelles and numerous regular mitochondria. Continuous exposure to CNC gel (Fig. 1B–C) or powder (Fig. 1D–E) for 4-weeks caused phenotypic changes as demonstrated by high number of cytoplasmic vacuoles with basophilic membrane-like materials, surface finger-like protrusions and multi-nucleation. In our previous publication (Menas et al., 2017) we reported that CNC powder and gel were taken up by the cells as was indicated by specific cellulose staining. On the other hand, TF are internalized by the cells as demonstrated in Fig. 1F–G and mostly visible in the cytoplasmic vacuoles. Additionally, sub-chronic exposure to TF for 4-weeks caused phenotypic changes as demonstrated by high number of cytoplasmic vacuoles and surface finger-like protrusions.

To assess CNC potential for neoplastic-like transformation, the colony forming efficiency (CFE) and *in vitro* cell transformation assay (CTA) were performed. BEAS-2B cells survived sub-chronic exposure to CNC or TF demonstrated significantly higher CFE and morphological transformation as evidenced by number of Type III foci compared to control cells (Fig. 2). Exposure to CNC powder or gel and TF induced 33%, 18% and 30% increase in CFE of BEAS-2B cells, respectively (Fig. 2A). Numbers of transformed foci, in particular Type III foci, were elevated by 1.71-, 2.47- and 5.03-folds of control after exposure to CNC powder or gel and TF, respectively (Fig. 2B). Type III foci exhibited deep basophilic staining and multilayering along with different cell orientations and invasive growth at colony edges (Fig. 2D–E).

3.4. Cell migration and invasion

To further investigate the potential aggressive behavior of cells continuously exposed to CNC or TF, BEAS-2B cells were evaluated for their chemotactic migration and invasion ability using Matrigel coated transwell inserts. Following long-term CNC powder, gel and TF exposure, BEAS-2B cells showed significantly higher migration rates (by 133%, 95%

and 45%, respectively) and enhanced ability to invade through matrix (by 30%, 29% and 103%, respectively) compared to control cells (Fig. 3).

3.5. Soft agar colony formation

The CNC or TF potential for neoplastic-like transformation of BEAS-2B cells was further assessed by measuring anchorage-independent cell growth on soft agar (Borowicz et al., 2014) (Fig. 4). A significant increase in the total number of colonies formed on soft agar was found following long-term exposure to.

CNC powder (by 75%), CNC gel (by 66%) or TF (by 152%) compared to control (p < 0.05; Fig. 4), thus suggesting an increased ability for anchorage-independent growth of BEAS-2B cells following long-term exposure to CNC or TF.

3.6. Cell apoptosis

Apoptosis analysis was performed using Cell Meter TUNEL assay kit. Long-term exposure of BEAS-2B cells to CNC powder or gel did not produce significant changes in apoptosis (Fig. S3) as compared to control cells.

3.7. Oxidative stress markers

The oxidative damage caused by 4-weeks of continuous exposure to CNC was assessed by measuring GSH/SH, oxidatively modified protein carbonyl and lipid peroxidation products in the cell lysates (Table S2). The levels of GSH in BEAS-2B cells were significantly depleted by 30% and 21%, following exposure to CNC powder or gel, respectively. The level of lipid peroxidation products, measured as HNE-His adducts, was significantly elevated (by 12%) only after CNC power exposure. No significant changes in the levels of protein-SH and oxidatively modified protein carbonyls were found after exposure to any of tested CNC (Table S2).

3.8. CNC-induced mediators of inflammation

The release of inflammatory cytokines with a subset of chemokine's/growth factors in cell supernatants was assessed following 4 weeks of BEAS-2B cells exposure with CNC, powder or gel, and TF. Significant release of twelve inflammatory cytokines (IL-1β, IL-2, IL-4, IL-9, eotaxin, IL-1ra, IL-6, IL-8, G-CSF, IP-10, IL-15 and TNF-α) was detected only when BEAS-2B cells were exposed to CNC powder while CNC gel-exposure significantly reduces secretion of RANTES (Table S3). Production of PDGF-bb was significantly diminished by both CNC powder and gel. Exposure to TF resulted in significant release of twenty inflammatory cytokines/chemokines. Seven of those (IL-5, IL-12p70, IL-13, IL-17, FGF-basic, GM-CSF and VEGF) are unique for TF exposure (Table S4).

3.9. Hierarchical clustering analysis

To further identify the patterns of cytokine secretion and their relationship to the different types of CNC exposures, hierarchical clustering analysis (HCA) was performed on the $\log_2$ transformed significant fold-change values of cytokines of CNC powder, - gel, and control samples (Fig. 5). Based on the HCA of the inflammatory cytokine responses, CNC powder exposure was found to be segregated from the control and CNC-gel samples (Fig. 5). This

suggests that the pro-inflammatory responses are more prominent upon treating BEAS-2B cells with CNC powder as compared to CNC gel and control. Moreover, the dendrogram on the left and top of the heatmap shows the intergroup dissimilarity between the samples as well as the different clusters of inflammatory cytokines. In the case of inflammatory cytokines, three distinct sub-groups: (1) IP-10, G-CSF, TNF-α, IL-1rα and RANTES; (2) IL-4, IL-2, Eotaxin, IL-1β, IL-15, and IL-9; (3) IL-8 and IL-6 were found to segregate BEAS-2B cells exposed to CNC powder, and - gel from control BEAS-2B cells (Fig. 5). These results suggest that biological responses in BEAS-2B cells upon exposure to CNC, gel and powder can be separated based on the cytokines data.

4. Discussion

NC is gaining popularity in different fields and the number of products containing those in the market is constantly growing, which can be explained by its unique physical characteristics, low cost and "green" properties such as being carbon neutral, sustainable, recyclable and renewable. The lack of knowledge regarding safety issues and health implications of NC exposure sets back further industrial and technological development (Iavicoli et al., 2017). To date, only a few publications have investigated the NC toxicity. Most of the studies employed short-term exposures (Shatkin and Kim, 2015) while understanding of the impact of chronic, repeated exposure on human health remains limited (Endes et al., 2016). This study aims to assess the ability of two different commercial forms of CNC to induce the neoplastic-like transformation in human bronchial epithelial (BEAS-2B) cells. Since CNC may be inhaled during various stages of their life-cycle (Clift et al., 2011), we employed sub-chronic repeated exposure model. Our results indicate that cell exposure to both gel and powder forms of CNC may potentially lead to neoplastic-like transformation of bronchial epithelial cells. Notably, the exposure effects were dependent on the type of CNC formulation i.e., gel versus powder form.

Carcinogenesis is a multi-step process that involves increased invasion and migration of cells, resistance to apoptosis, cell proliferation, and angiogenesis (Hanahan and Weinberg, 2000; Gatenby and Gillies, 2008). In this study, continuous long-term exposure of BEAS-2B cells to CNC ($30 \, \mu g/cm^2$) induced increased anchorage independent growth, formation of Type-III foci and augmented cell migration and invasion (Figs. 2–4). The migration of normal cells is often tightly regulated. However, cells with a cancer-like phenotype or derived from tumors, are known to promote migration/invasion due to their modified microenvironments. Noncancerous BEAS-2B cells exposed to either CNC-powder or -gel showed higher migration rates compared to non-exposed control cells. The hierarchy of such responses were also in good agreement with the elevated IL-6 and IL-8 cytokine levels (Table S3, Fig. 5), known to promote cell migration and invasion (Waugh and Wilson, 2008; Lang et al., 2002). The increased levels of IL-1β in CNC powder exposed BEAS-2B cells (Fig. 5, Table S3), were also in line with the increased cellular migration and invasiveness phenotype (White et al., 2008). While cellular invasion is related to and encompasses migration, invasion of cells into neighboring tissues requires the degradation of extracellular matrix (Shian et al., 2003). Cell invasion is critical for both normal and pathological processes including immune response and metastatic growth.

A growing body of evidence suggests that chronic inflammation contributes to cancer development and progression as it triggers various pathological processes that may lead to neoplastic transformation (Balkwill and Mantovani, 2001; Coussens and Werb, 2001; Lu et al., 2006; Pine et al., 2011; Landskron et al., 2014). Chronic inflammation can be the cause or result of cellular oxidative stress. We found that exposure to both forms of CNC for 72 h induced generation of intracellular ROS (Fig. S2B) while continuous long-term exposure resulted in significant depletion of GSH level (Table S2). In contrast, accumulation of lipid peroxidation product (HNE-His protein adducts) was induced only by CNC powder (Table S2). A moderate increase in ROS can promote cell proliferation and differentiation (Boonstra and Post, 2004; Schafer and Buettner, 2001), whereas excessive amounts of ROS can cause oxidative damage. An increase in ROS is known to be associated with abnormal cancer cell growth and reflects a disruption of redox homeostasis due either to an elevation of ROS production or to a decline of ROS-scavenging capacity (Toyokuni et al., 1995). These pro-oxidant manifestations were also accompanied by complex changes in the levels of various cytokines and chemokines related to inflammation and/or angiogenesis (Table S3). For instance, exposure of BEAS-2B cells to CNC powder induced accumulation of TNF-α, known to be elevated in the early stages of carcinogenesis, including angiogenesis and invasion (Moore et al., 1999; Szlosarek et al., 2006). A TNF-α tumor promotion mechanism is based on ROS generation, which can induce DNA damage, hence facilitate tumorigenesis (Woo et al., 2000; Hussain et al., 2003). Exposure to CNC, powder or gel, for 72 h resulted in the increased DNA damage (Fig. S2C) that is in line with elevated ROS production (Fig. S2C). Similarly, previous studies reported an induction of DNA strand breaks by NC *in vitro* as well as *in vivo* (Catalan et al., 2017; de Lima et al., 2012). However, the exposure effect varied significantly between CNC forms: CNC-powder altered the secretion levels of pro- and anti-inflammatory cytokines including IL-6, MCP-1, TNF-α, eotaxin, IL-1rα etc.; whereas exposure to CNC-gel affected the expression level of RANTES only. In addition, 4 weeks of exposure to CNC powder or gel induced morphological changes in cells (Fig. 1). CNC powder and gel particles uptake were demonstrated in our earlier publication (Menas et al., 2017). In line with these results, Wang et al. (2019) showed length-dependent uptake of FITC-labeled CNC and their co-localization with lysosomes as well as inflammatory response and ROS generation. Thus, slightly larger widths and hydrodynamic diameters (Table S1) of CNC powder in our study might be important for the enhanced cellular/inflammatory responses.

Moreover, a significant upregulation of IL-4, IL-6 and IL-8 seen in BEAS-2B cells upon exposure to CNC powder (Table S3, Fig. 5) may provide a favorable microenvironment for increased cell proliferation (Nappo et al., 2017; Tsai et al., 2014). Thus, BEAS-2B cells continuously exposed to CNC exhibited significantly increased proliferation demonstrated by amplified CFE, anchorage independent growth in soft agar and the total number of foci per plate, in particular Type III (Figs. 2 and 4). Enhanced CFE and elevated levels of invasive Type III foci on a confluent monolayer suggest a possibility of morphological transformation (Ponti et al., 2013; Sasaki et al., 2012).

To evaluate and determine the extent of inflammatory responses and the cell neoplastic potential induced by CNC, respirable tremolite asbestos fibers were investigated for comparison. A growing body of evidence suggests that tremolite fibers could be important in

the pathogenesis of lung tumors (Pugnaloni et al., 2013). Considerable epidemiological data on tremolite asbestos are related to mesothelioma, a malignant tumor of the pleura or peritoneum (McDonald, 2010; Rudd, 2010). Our findings indicate that exposure of BEAS-2B cells to TF (2.5 μg/cm^2) resulted in intracellular ROS generation and DNA damage (Figs. S2B–C), particle uptake and cells morphological changes (Fig. 1). Moreover, TF caused an increase in anchorage independent growth, formation of Type-III foci, colony formation and augmented cell migration and invasion (Figs. 2–4). Also, it is important to mention that TF exposure lead to the significant release of twenty specific inflammatory cytokines/chemokines/growth factors (Table S4). However, not only similar but also distinctive differences in response were found compare to CNC exposure. Seven of those mediators (IL-5, IL-12p70, IL-13, IL-17, FGF-basic, GM-CSF and VEGF) were unique for TF exposure cells as compared to CNC. These results are in line with already published, demonstrating elevation of several cytokines that have been implicated in asbestos (including tremolite) carcinogenesis, such as IL-17, IL-6, IL-8, VEGF, PDGF (Zebedeo et al., 2014; Yang et al., 2008; Pugnaloni et al., 2013). Numerous studies have shown that IL-17 promotes tumor angiogenesis, cell proliferation and higher invasiveness therefore contributes to the progression of lung cancer (Wu et al., 2016; Yang et al., 2014). The potent role of VEGF in tumor angiogenesis has been widely described in the last decade. VEGF is expressed in most tumors and its expression correlates with tumor progression (Costache et al., 2015). Moreover, increased secretion of VEGF through IL-17 dependent mechanism was reported to be a factor worsening cancer patients' prognoses (Liu et al., 2011). FGF is allied with multiple biological activities including cellular proliferation, differentiation, invasiveness and motility that demonstrate the potential to initiate and promote tumorigenesis (Korc and Friesel, 2009). Besides, recent studies have shown that FGF can act synergistically with VEGF to amplify tumor angiogenesis (Giavazzi et al., 2003). A large body of experimental evidence indicates that GM-CSF promotes tumor progression by supporting tumor microenvironment and stimulating tumor growth and/or metastasis (Hong, 2016). In addition, IL-13 known to mediate biological effects, such as tumor proliferation, cell survival and metastasis. In certain cancers, the presence of these cytokines' receptors may serve as biomarkers of cancer aggressiveness (Suzuki et al., 2015). Likewise, it was demonstrated that IL-5 could directly promote migration and invasion of cancer cells (Lee et al., 2013). Increased expression of IL-5 in some carcinomas has been linked to the higher rates of development of distant metastasis and poor prognosis (Eiro et al., 2012). Similarly, IL-12, a powerful inducer of Th1 responses and an antitumor cytokine in cancer diseases, was found abnormally elevated in some metastatic cancers thus associating with disease progression (Kovacs, 2001). Our data suggest that the exposure to CNC and TF may induce distinct responses in BEAS-2B cells. While CNC exposure resulted in some similar outcomes, TF induce stronger as well as unique responses.

Organization for Economic Co-operation and Development (OECD) guidelines state that a combined analysis of anchorage independent growth, CFE and Type III foci is a powerful tool to investigate the morphological neoplastic transformation induced by both genotoxic and non-genotoxic carcinogens *in vitro* (Vasseur and Lasne, 2012; OECD, 2007). Thus, the enhanced colony forming efficiency, augmented cellular migration and invasion together with increased Type III foci per plate observed in CNC exposed noncancerous BEAS-2B

cells highlights CNC's potential to trigger cellular transformation events *in vitro*. However, further studies focusing on the genotoxic and non-genotoxic responses would be critical to understand how CNC exposure can trigger such responses *in vitro* model.

5. Conclusion

In summary, our results provide novel information compatible with the potential neoplastic-like transformation effect of CNC *in vitro*. Our findings show that gel and powder CNC affect cells differently, leading to distinct alterations in cellular responses including variations in secretion patterns of various pro- and anti-inflammatory cytokines, chemokines, and growth factors. Observed outcome variations indicate that the cellular transformation ability of CNC may be dependent on the production technology, which can affect the particle characteristics and structural configuration of CNCs produced. The biological processes underlying these differences across the CNC forms/type are intriguing and need to be studied in more detail. There are intrinsic limitations present, that one should be aware of, when conducting *in vitro* study that aims at assessing potential carcinogenic outcomes. For example, single cell type model lacks the complexity inherent to a whole organism, however, the mechanisms responsible for potential cellular transformation are robust and on an organism level even a single cell neoplastic transformation event, if left unchecked, may lead to a neoplasia. One should also bear in mind that the cytokine milieu in lungs is created through the contribution of numerous cell subsets, particularly immune cells, nevertheless, bronchial epithelial cells are also a major player in the immune response regulation and can even initiate inflammatory cascades through secretion of bioactive molecules (Levine, 1995; Pfeffer et al., 2018). In addition, our findings are limited to the type of nanocellulose particles, cell-type and conditions investigated, and great care should be taken when generalizing them to other types of CNC, isolated from different sources and through different extraction and fabrication methods.

Supplementary Material

Refer to Web version on PubMed Central for supplementary material.

Acknowledgments

References

Aierken D, Okazaki Y, Chew SH, Sakai A, Wang Y, Nagai H, Misawa N, Kohyama N, Toyokuni S, 2014 Rat model demonstrates a high risk of tremolite but a low risk of anthophyllite for mesothelial carcinogenesis. Nagoya J. Med. Sci 76 (1–2), 149–160. [PubMed: 25130001]

Athanasiou K, Constantopoulos SH, Rivedal E, Fitzgerald DJ, Yamasaki H, 1992 Metsovo-tremolite asbestos fibres: in vitro effects on mutation, chromosome aberration, cell transformation and intercellular communication. Mutagenesis 7 (5), 343–347. 10.1093/mutage/7.5.343. [PubMed: 1470029]

Balkwill F, Mantovani A, 2001 Inflammation and cancer: back to Virchow? Lancet 357 (9255), 539–545. 10.1016/S0140-6736(00)04046-0. [PubMed: 11229684]

Bocchetta M, Di Resta I, Powers A, Fresco R, Tosolini A, Testa JR, Pass HI, Rizzo P, Carbone M, 2000 Human mesothelial cells are unusually susceptible to simian virus 40-mediated transformation and asbestos cocarcinogenicity. Proc. Natl. Acad. Sci. U. S. A 97 (18), 10214–10219. 10.1073/pnas.170207097. [PubMed: 10954737]

Boonstra J, Post JA, 2004 Molecular events associated with reactive oxygen species and cell cycle progression in mammalian cells. Gene 337,1–13. 10.1016/j.gene.2004.04.032. [PubMed: 15276197]

Borowicz S, Van Scoyk M, Avasarala S, Karuppusamy Rathinam MK, Tauler J, Bikkavilli RK, Winn RA, 2014 The soft agar colony formation assay. J Vis Exp 92, e51998 10.3791/51998.

Bradford MM, 1976 A rapid and sensitive method for the quantitation of microgram quantities of protein utilizing the principle of protein-dye binding. Anal. Biochem 72, 248–254. 10.1006/abio.1976.9999. [PubMed: 942051]

Catalan J, Ilves M, Jarventaus H, Hannukainen KS, Kontturi E, Vanhala E, Alenius H, Savolainen KM, Norppa H, 2015 Genotoxic and immunotoxic effects of cellulose nanocrystals in vitro. Environ. Mol. Mutagen 56 (2), 171–182. 10.1002/em.21913. [PubMed: 25257801]

Catalan J, Rydman E, Aimonen K, Hannukainen KS, Suhonen S, Vanhala E, Moreno C, Meyer V, Perez DD, Sneck A, Forsstrom U, Hojgaard C, Willemoes M, Winther JR, Vogel U, Wolff H, Alenius H, Savolainen KM, Norppa H, 2017 Genotoxic and inflammatory effects of nanofibrillated cellulose in murine lungs. Mutagenesis 32 (1), 23–31. 10.1093/mutage/gew035. [PubMed: 27470699]

Chen BT, Schwegler-Berry D, McKinney W, Stone S, Cumpston JL, Friend S, Porter DW, Castranova V, Frazer DG, 2012 Multi-walled carbon nanotubes: sampling criteria and aerosol characterization. Inhal. Toxicol 24 (12), 798–820. 10.3109/08958378.2012.720741. [PubMed: 23033994]

Clift MJ, Foster EJ, Vanhecke D, Studer D, Wick P, Gehr P, Rothen-Rutishauser B, Weder C, 2011 Investigating the interaction of cellulose nanofibers derived from cotton with a sophisticated 3D human lung cell coculture. Biomacromolecules 12 (10), 3666–3673. 10.1021/bm200865j. [PubMed: 21846085]

Costache MI, Ioana M, Iordache S, Ene D, Costache CA, Saftoiu A, 2015 VEGF expression in pancreatic cancer and other malignancies: a review of the literature. Rom. J. Intern. Med 53 (3), 199–208. 10.1515/rjim-2015-002.

Coussens LM, Werb Z, 2001 Inflammatory cells and cancer: think different! J. Exp. Med 193 (6), F23–F26. [PubMed: 11257144]

Creton S, Aardema MJ, Carmichael PL, Harvey JS, Martin FL, Newbold RF, O'Donovan MR, Pant K, Poth A, Sakai A, Sasaki K, Scott AD, Schechtman LM, Shen RR, Tanaka N, Yasaei H, 2012 Cell transformation assays for prediction of carcinogenic potential: state of the science and future research needs. Mutagenesis 27 (1), 93–101. 10.1093/mutage/ger053. [PubMed: 21852270]

Cullen RT, Searl A, Miller BG, Davis JM, Jones AD, 2000 Pulmonary and intraperitoneal inflammation induced by cellulose fibres.J. Appl. Toxicol 20(1), 49–60. [PubMed: 10641016]

Davis JM, Addison J, McIntosh C, Miller BG, Niven K, 1991 Variations in the carcinogenicity of tremolite dust samples of differing morphology. Ann. N. Y. Acad. Sci 643, 473–490. 10.1111/j.1749-6632.1991.tb24497.x. [PubMed: 1809161]

de Lima R, Oliveira Feitosa L, Rodrigues Maruyama C, Abreu Barga M, Yamawaki PC, Vieira IJ, Teixeira EM, Correa AC, Caparelli Mattoso LH, Fernandes Fraceto L, 2012 Evaluation of the genotoxicity of cellulose nanofibers. Int. J. Nanomed 7, 3555–3565. 10.2147/IJN.S30596.

Ede JD, Ong KJ, Goergen M, Rudie A, Pomeroy-Carter CA, Shatkin JA, 2019 Risk analysis of cellulose nanomaterials by inhalation: current state of science. Nanomaterials 9 (3). 10.3390/nano9030337.

Eiro N, Gonzalez L, Gonzalez LO, Fernandez-Garcia B, Lamelas ML, Marin L, Gonzalez-Reyes S, del Casar JM, Vizoso FJ, 2012 Relationship between the inflammatory molecular profile of breast carcinomas and distant metastasis development. PloS One 7 (11), e49047 10.1371/journal.pone.0049047. [PubMed: 23145063]

Endes C, Camarero-Espinosa S, Mueller S, Foster EJ, Petri-Fink A, Rothen-Rutishauser B, Weder C, Clift MJ, 2016 A critical review of the current knowledge regarding the biological impact of nanocellulose. J. Nanobiotechnol 14 (1), 78 10.1186/s12951-016-0230-9.

Endes C, Schmid O, Kinnear C, Mueller S, Camarero-Espinosa S, Vanhecke D, Foster EJ, Petri-Fink A, Rothen-Rutishauser B, Weder C, Clift MJ, 2014 An in vitro testing strategy towards mimicking the inhalation of high aspect ratio nanoparticles. Part. Fibre Toxicol 11, 40 10.1186/s12989-014-0040-x. [PubMed: 25245637]

Gatenby RA, Gillies RJ, 2008 A microenvironmental model of carcinogenesis. Nat. Rev. Canc 8 (1), 56–61. 10.1038/nrc2255.

Giavazzi R, Sennino B, Coltrini D, Garofalo A, Dossi R, Ronca R, Tosatti MP, Presta M, 2003 Distinct role of fibroblast growth factor-2 and vascular endothelial growth factor on tumor growth and angiogenesis. Am. J. Pathol 162 (6), 1913–1926. 10.1016/S0002-9440(10)64325-8. [PubMed: 12759248]

Hanahan D, Weinberg RA, 2000 The hallmarks of cancer. Cell 100 (1), 57–70. [PubMed: 10647931]

Hanahan D, Weinberg RA, 2011 Hallmarks of cancer: the next generation. Cell 144 (5), 646–674. 10.1016/j.cell.2011.02.013. [PubMed: 21376230]

Harper Martin, Bradley Van Gosen, Crankshaw Owen S., Doorn Stacy S., Ennis Todd J., Harrison Sara E., 2014 Characterization of lone pine, California, tremolite asbestos and preparation of research material. Annals of Work Exposures and Health 59 (1), 91–103. 10.1093/annhyg/meu074. % J Annals of Work Exposures and Health.

Hong IS, 2016 Stimulatory versus suppressive effects of GM-CSF on tumor progression in multiple cancer types. Exp. Mol. Med 48 (7), e242 10.1038/emm.2016.64. [PubMed: 27364892]

Howard J, Murashov V, 2009 National nanotechnology partnership to protect workers. J. Nanoparticle Res 11 (7), 1673–1683. 10.1007/s11051-009-9682-2.

Hussain SP, Hofseth LJ, Harris CC, 2003 Radical causes of cancer. Nat. Rev. Cancer 3, 276–285. [PubMed: 12671666]

Iavicoli I, Leso V, Beezhold DH, Shvedova AA, 2017 Nanotechnology in agriculture: opportunities, toxicological implications, and occupational risks. Toxicol. Appl. Pharmacol 329, 96–111. 10.1016/j.taap.2017.05.025. [PubMed: 28554660]

Joseph P, Umbright C, Sager T, Chen T, McKinney W, Orandle M, Roberts J, 2017 Pulmonary toxicity in response to inhalation exposure to nanocrystalline cellulose in the rat.

Ke Y, Reddel RR, Gerwin BI, Miyashita M, McMenamin M, Lechner JF, Harris CC, 1988 Human bronchial epithelial cells with integrated SV40 virus T antigen genes retain the ability to undergo squamous differentiation. Differentiation 38 (1), 60–66. [PubMed: 2846394]

Klein-Szanto AJ, Iizasa T, Momiki S, Garcia-Palazzo I, Caamano J, Metcalf R, Welsh J, Harris CC, 1992 A tobacco-specific N-nitrosamine or cigarette smoke condensate causes neoplastic transformation of xenotransplanted human bronchial epithelial cells. Proc. Natl. Acad. Sci. U. S. A 89 (15), 6693–6697. [PubMed: 1323115]

Kohyama N, Fujiki M, Kishimoto T, Morinaga K, 2017 Lung cancer in a patient with predominantly short tremolite fibers in his lung. Am. J. Ind. Med 60 (9), 831–838. 10.1002/ajim.22748. [PubMed: 28744908]

Korc M, Friesel RE, 2009 The role of fibroblast growth factors in tumor growth. Curr. Cancer Drug Targets 9 (5), 639–651. [PubMed: 19508171]

Kovacs E, 2001 The serum levels of IL-12 and IL-16 in cancer patients. Relation to the tumour stage and previous therapy. Biomed. Pharmacother 55 (2), 111–116. [PubMed: 11293814]

Landskron G, De la Fuente M, Thuwajit P, Thuwajit C, Hermoso MA, 2014 Chronic inflammation and cytokines in the tumor microenvironment. J Immunol Res 2014,149185 10.1155/2014/149185. [PubMed: 24901008]

Lang K, Niggemann B, Zanker KS, Entschladen F, 2002 Signal processing in migrating T24 human bladder carcinoma cells: role of the autocrine interleukin-8 loop. Int. J. Canc 99 (5), 673–680. 10.1002/ijc.10424.

Lee EJ, Lee SJ, Kim S, Cho SC, Choi YH, Kim WJ, Moon SK, 2013 Interleukin-5 enhances the migration and invasion of bladder cancer cells via ERK1/2-mediated MMP-9/NF-kappaB/AP-1 pathway: involvement of the p21WAF1 expression. Cell. Signal. 25 (10), 2025–2038. 10.1016/j.cellsig.2013.06.004. [PubMed: 23770289]

Levine SJ, 1995 Bronchial epithelial cell-cytokine interactions in airway inflammation. J. Invest. Med 43 (3), 241–249.

Liu J, Duan Y, Cheng X, Chen X, Xie W, Long H, Lin Z, Zhu B, 2011 IL-17 is associated with poor prognosis and promotes angiogenesis via stimulating VEGF production of cancer cells in colorectal carcinoma. Biochem. Biophys. Res. Commun 407 (2), 348–354. 10.1016/j.bbrc.2011.03.021. [PubMed: 21396350]

Lu H, Ouyang W, Huang C, 2006 Inflammation, a key event in cancer development. Mol. Canc. Res 4 (4), 221–233. 10.1158/1541-7786.MCR-05-0261.

McDonald JC, 2010 Epidemiology of malignant mesothelioma-an outline. Ann. Occup. Hyg 54 (8), 851–857. 10.1093/annhyg/meq076. [PubMed: 21059834]

Menas AL, Yanamala N, Farcas MT, Russo M, Friend S, Fournier PM, Star A, Iavicoli I, Shurin GV, Vogel UB, Fadeel B, Beezhold D, Kisin ER, Shvedova AA, 2017 Fibrillar vs crystalline nanocellulose pulmonary epithelial cell responses: cytotoxicity or inflammation? Chemosphere 171, 671–680. 10.1016/j.chemosphere.2016.12.105. [PubMed: 28061425]

Moore RJ, Owens DM, Stamp G, Arnott C, Burke F, East N, Holdsworth H, Turner L, Rollins B, Pasparakis M, Kollias G, Balkwill F, 1999 Mice deficient in tumor necrosis factor-alpha are resistant to skin carcinogenesis. Nat. Med 5 (7), 828–831. 10.1038/10552. [PubMed: 10395330]

Nappo G, Handle F, Santer FR, McNeill RV, Seed RI, Collins AT, Morrone G, Culig Z, Maitland NJ, Erb HHH, 2017 The immunosuppressive cytokine interleukin-4 increases the clonogenic potential of prostate stem-like cells by activation of STAT6 signalling. Oncogenesis 6 (5), e342 10.1038/oncsis.2017.23. [PubMed: 28553931]

Nygren J, Suhonen S, Norppa H, Linnainmaa K, 2004 DNA damage in bronchial epithelial and mesothelial cells with and without associated crocidolite asbestos fibers. Environ. Mol. Mutagen 44 (5), 477–482. 10.1002/em.20066. [PubMed: 15534864]

Oberdorster G, 2010 Safety assessment for nanotechnology and nanomedicine: concepts of nanotoxicology. J. Intern. Med 267 (1), 89–105. 10.1111/j.1365-2796.2009.02187.x. [PubMed: 20059646]

OECD, 2007 Detailed review paper on cell transformation assays for detection of chemical carcinogens In: Series on Testing and Assessment. OECD, Paris, France.

Ollikainen T, Linnainmaa K, Kinnula VL, 1999 DNA single strand breaks induced by asbestos fibers in human pleural mesothelial cells in vitro. Environ. Mol. Mutagen 33 (2), 153–160. [PubMed: 10217069]

Österberg M, Cranston ED, 2014 Special issue on nanocellulose- Editorial. In: Nordic Pulp & Paper Research Journal.

Park EJ, Khaliullin TO, Shurin MR, Kisin ER, Yanamala N, Fadeel B, Chang J, Shvedova AA, 2018 Fibrous nanocellulose, crystalline nanocellulose, carbon nanotubes, and crocidolite asbestos elicit disparate immune responses upon pharyngeal aspiration in mice. J. Immunot 15 (1), 12–23. 10.1080/1547691X.2017.1414339.

Park SH, 2018 Types and health hazards of fibrous materials used as asbestos substitutes. Saf Health Work 9 (3), 360–364. 10.1016/j.shaw.2018.05.001. [PubMed: 30370171]

Park YH, Kim D, Dai J, Zhang Z, 2015 Human bronchial epithelial BEAS-2B cells, an appropriate in vitro model to study heavy metals induced carcinogenesis. Toxicol. Appl. Pharmacol 287 (3), 240–245. 10.1016/j.taap.2015.06.008. [PubMed: 26091798]

Pfeffer PE, Lu H, Mann EH, Chen YH, Ho TR, Cousins DJ, Corrigan C, Kelly FJ, Mudway IS, Hawrylowicz CM, 2018 Effects of vitamin D on inflammatory and oxidative stress responses of human bronchial epithelial cells exposed to particulate matter. PloS One 13 (8), e0200040 10.1371/journal.pone.0200040. [PubMed: 30157189]

Pine SR, Mechanic LE, Enewold L, Chaturvedi AK, Katki HA, Zheng YL, Bowman ED, Engels EA, Caporaso NE, Harris CC, 2011 Increased levels of circulating interleukin 6, interleukin 8, C-reactive protein, and risk of lung cancer. J. Natl. Cancer Inst 103 (14), 1112–1122. 10.1093/jnci/djr216. [PubMed: 21685357]

Ponti J, Broggi F, Mariani V, De Marzi L, Colognato R, Marmorato P, Gioria S, Gilliland D, Pascual Garcia C, Meschini S, Stringaro A, Molinari A, Rauscher H, Rossi F, 2013 Morphological transformation induced by multiwall carbon nanotubes on Balb/3T3 cell model as an in vitro end point of carcinogenic potential. Nanotoxicology 7 (2), 221–233. 10.3109/17435390.2011.652681. [PubMed: 22279961]

Pugnaloni A, Giantomassi F, Lucarini G, Capella S, Bloise A, Di Primio R, Belluso E, 2013 Cytotoxicity induced by exposure to natural and synthetic tremolite asbestos: an in vitro pilot study. Acta Histochem. 115 (2), 100–112. 10.1016/j.acthis.2012.04.004. [PubMed: 22578742]

Qi F, Okimoto G, Jube S, Napolitano A, Pass HI, Laczko R, Demay RM, Khan G, Tiirikainen M, Rinaudo C, Croce A, Yang H, Gaudino G, Carbone M, 2013 Continuous exposure to chrysotile asbestos can cause transformation of human mesothelial cells via HMGB1 and TNF-alpha signaling. Am. J. Pathol 183 (5), 1654–1666. 10.1016/j.ajpath.2013.07.029. [PubMed: 24160326]

R Core Team, 2014 R: A Language and Environment for Statistical Computing. R Foundation for Statistical Computing, Vienna, Austria https://www.R-project.org/.

Roggli VL, Vollmer RT, Butnor KJ, Sporn TA, 2002 Tremolite and mesothelioma. Ann. Occup. Hyg 46 (5), 447–453. [PubMed: 12176759]

Roman Maren, 2015 Toxicity of cellulose nanocrystals: a review. Ind. Biotechnol 11 (1), 25–33. 10.1089/ind.2014.0024.

Rudd RM, 2010 Malignant mesothelioma. Br. Med. Bull 93, 105–123. 10.1093/bmb/ldp047. [PubMed: 20047972]

Sasaki K, Bohnenberger S, Hayashi K, Kunkelmann T, Muramatsu D, Poth A, Sakai A, Salovaara S, Tanaka N, Thomas BC, Umeda M, 2012 Photo catalogue for the classification of foci in the BALB/c 3T3 cell transformation assay. Mutat. Res 744 (1), 42–53. 10.1016/j.mrgentox.2012.01.009. [PubMed: 22331008]

Schafer FQ, Buettner GR, 2001 Redox environment of the cell as viewed through the redox state of the glutathione disulfide/glutathione couple. Free Radic. Biol. Med 30 (11), 1191–1212. 10.1016/s0891-5849(01)00480-4. [PubMed: 11368918]

Schneider J, Rodelsperger K, Bruckel B, Kayser K, Woitowitz HJ, 1998 Environmental exposure to tremolite asbestos: pleural mesothelioma in two Turkish workers in Germany. Rev. Environ. Health 13 (4), 213–220. [PubMed: 9987816]

Shatkin JA, Kim B, 2015 Cellulose nanomaterials: life cycle risk assessment, and environmental health and safety roadmap. Environ. Sci. J. Integr. Environ. Res.: Nano 2 (5), 477–499. 10.1039/C5EN00059A.

Shian SG, Kao YR, Wu FY, Wu CW, 2003 Inhibition of invasion and angiogenesis by zinc-chelating agent disulfiram. Mol. Pharmacol 64 (5), 1076–1084. 10.1124/mol.64.5.1076. [PubMed: 14573756]

Shvedova AA, Kisin ER, Yanamala N, Farcas MT, Menas AL, Williams A, Fournier PM, Reynolds JS, Gutkin DW, Star A, Reiner RS, Halappanavar S, Kagan VE, 2016 Gender differences in murine pulmonary responses elicited by cellulose nanocrystals. Part. Fibre Toxicol 13 (1), 28 10.1186/s12989-016-0140-x. [PubMed: 27278671]

Srivastava RK, Lohani M, Pant AB, Rahman Q, 2010 Cyto-genotoxicity of amphibole asbestos fibers in cultured human lung epithelial cell line: role of surface iron. Toxicol. Ind. Health 26 (9), 575–582. 10.1177/0748233710374464. [PubMed: 20554628]

Stefaniak AB, Seehra MS, Fix NR, Leonard SS, 2014 Lung biodurability and free radical production of cellulose nanomaterials. Inhal. Toxicol 26 (12), 733–749. 10.3109/08958378.2014.948650. [PubMed: 25265049]

Suzuki A, Leland P, Joshi BH, Puri RK, 2015 Targeting of IL-4 and IL-13 receptors for cancer therapy. Cytokine 75 (1), 79–88. 10.1016/j.cyto.2015.05.026. [PubMed: 26088753]

Szlosarek P, Charles KA, Balkwill FR, 2006 Tumour necrosis factor-alpha as a tumour promoter. Eur. J. Canc 42 (6), 745–750. 10.1016/j.ejca.2006.01.012.

Toyokuni S, Okamoto K, Yodoi J, Hiai H, 1995 Persistent oxidative stress in cancer. FEBS Lett. 358 (1), 1–3. 10.1016/0014-5793(94)01368-b. [PubMed: 7821417]

Tsai MJ, Chang WA, Huang MS, Kuo PL, 2014 Tumor microenvironment: a new treatment target for cancer. ISRN Biochem 2014, 351959 10.1155/2014/351959. [PubMed: 25937967]

van Agen B, Maas LM, Zwingmann IH, Van Schooten FJ, Kleinjans JC, 1997 B[a]P-DNA adduct formation and induction of human epithelial lung cell transformation. Environ. Mol. Mutagen 30 (3), 287–292. [PubMed: 9366906]

Vasseur P, Lasne C, 2012 OECD detailed review paper (DRP) number 31 on "cell transformation assays for detection of chemical carcinogens": main results and conclusions. Mutat. Res 744 (1), 8–11. 10.1016/j.mrgentox.2011.11.007. [PubMed: 22120692]

Wang L, Stueckle TA, Mishra A, Derk R, Meighan T, Castranova V, Rojanasakul Y, 2014 Neoplastic-like transformation effect of single-walled and multi-walled carbon nanotubes compared to asbestos on human lung small airway epithelial cells. Nanotoxicology 8 (5), 485–507. 10.3109/17435390.2013.801089. [PubMed: 23634900]

Wang X, Chang CH,Jiang J, Liu Q, Liao YP, Lu J, Li L, Liu X, Kim J, Ahmed A, Nel AE, Xia T, 2019 The crystallinity and aspect ratio of cellulose nanomaterials determine their pro-inflammatory and immune adjuvant effects in vitro and in vivo. Small, e1901642 10.1002/smll.201901642. [PubMed: 31461215]

Waugh DJ, Wilson C, 2008 The interleukin-8 pathway in cancer. Clin. Canc. Res 14 (21), 6735–6741. 10.1158/1078-0432.CCR-07-4843.

White SR, Fischer BM, Marroquin BA, Stern R, 2008 Interleukin-1 beta mediates human airway epithelial cell migration via NF-kappaB. Am. J. Physiol. Lung Cell Mol. Physiol 295 (6), L1018–L1027. 10.1152/ajplung.00065.2008. [PubMed: 18849440]

Woo CH, Eom YW, Yoo MH, You HJ, Han HJ, Song WK, Yoo YJ, Chun JS, Kim JH, 2000 Tumor necrosis factor-alpha generates reactive oxygen species via a cytosolic phospholipase A2-linked cascade. J. Biol. Chem 275 (41), 32357–32362. [PubMed: 10934206]

Wu F, Xu J, Huang Q, Han J, Duan L, Fan J, Lv Z, Guo M, Hu G, Chen L, Zhang S, Tao X, Ma W, Jin Y, 2016 The role of interleukin-17 in lung cancer. Mediat. Inflamm 2016, 8494079 10.1155/2016/8494079.

Yanamala N, Farcas MT, Hatfield MK, Kisin ER, Kagan VE, Geraci CL, Shvedova AA, 2014 In vivo evaluation of the pulmonary toxicity of cellulose nanocrystals: a renewable and sustainable nanomaterial of the future. ACS Sustain. Chem. Eng 2 (7), 1691–1698. 10.1021/sc500153k.

Yanamala N, Kisin ER, Menas AL, Farcas MT, Khaliullin TO, Vogel UB, Shurin GV, Schwegler-Berry D, Fournier PM, Star A, Shvedova AA, 2016 In vitro toxicity evaluation of lignin-(Un)coated cellulose based nanomaterials on human A549 and THP-1 cells. Biomacromolecules 17 (11), 3464–3473. 10.1021/acs.biomac.6b00756. [PubMed: 27709894]

Yang B, Kang H, Fung A, Zhao H, Wang T, Ma D, 2014 The role of interleukin 17 in tumour proliferation, angiogenesis, and metastasis. Mediat. Inflamm 2014, 623759 10.1155/2014/623759.

Yang H, Testa JR, Carbone M, 2008 Mesothelioma epidemiology, carcinogenesis, and pathogenesis. Curr. Treat. Options Oncol 9 (2–3), 147–157. 10.1007/s11864-008-0067-z. [PubMed: 18709470]

Zebedeo CN, Davis C, Pena C, Ng KW, Pfau JC, 2014 Erionite induces production of autoantibodies and IL-17 in C57BL/6 mice. Toxicol. Appl. Pharmacol 275 (3), 257–264. 10.1016/j.taap.2014.01.018. [PubMed: 24518925]

HIGHLIGHTS

- CNC may have the ability to influence neoplastic-like transformation events.

- Proliferative responses are in agreement with levels of inflammatory cytokines.

- Exposure to CNC gel or powder leads to distinct alterations in cellular responses.

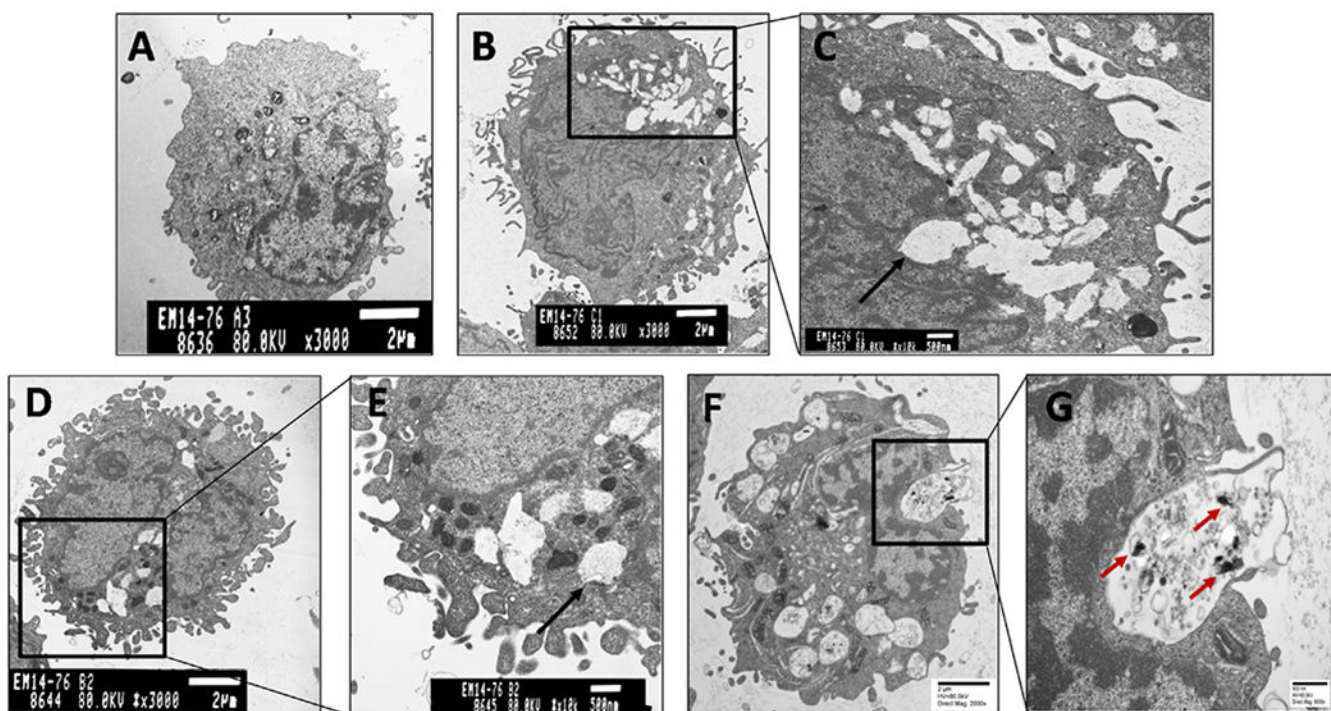- Distinctive differences in response were found after exposure to TF compare to CNC.

Fig. 1.
Representative TEM micrographs of BEAS-2B cells after 4 weeks (72 h/week) of exposure with CNC (30 μg/cm^2) or TF (2.5 μg/cm^2), where (A) control cells, (B–C) CNC gel-treated cells, (D–E) CNC powder-treated cells and (F–G) TF-exposed cells. Red arrows indicating visible particle uptake. (For interpretation of the references to color in this figure legend, the reader is referred to the Web version of this article.)
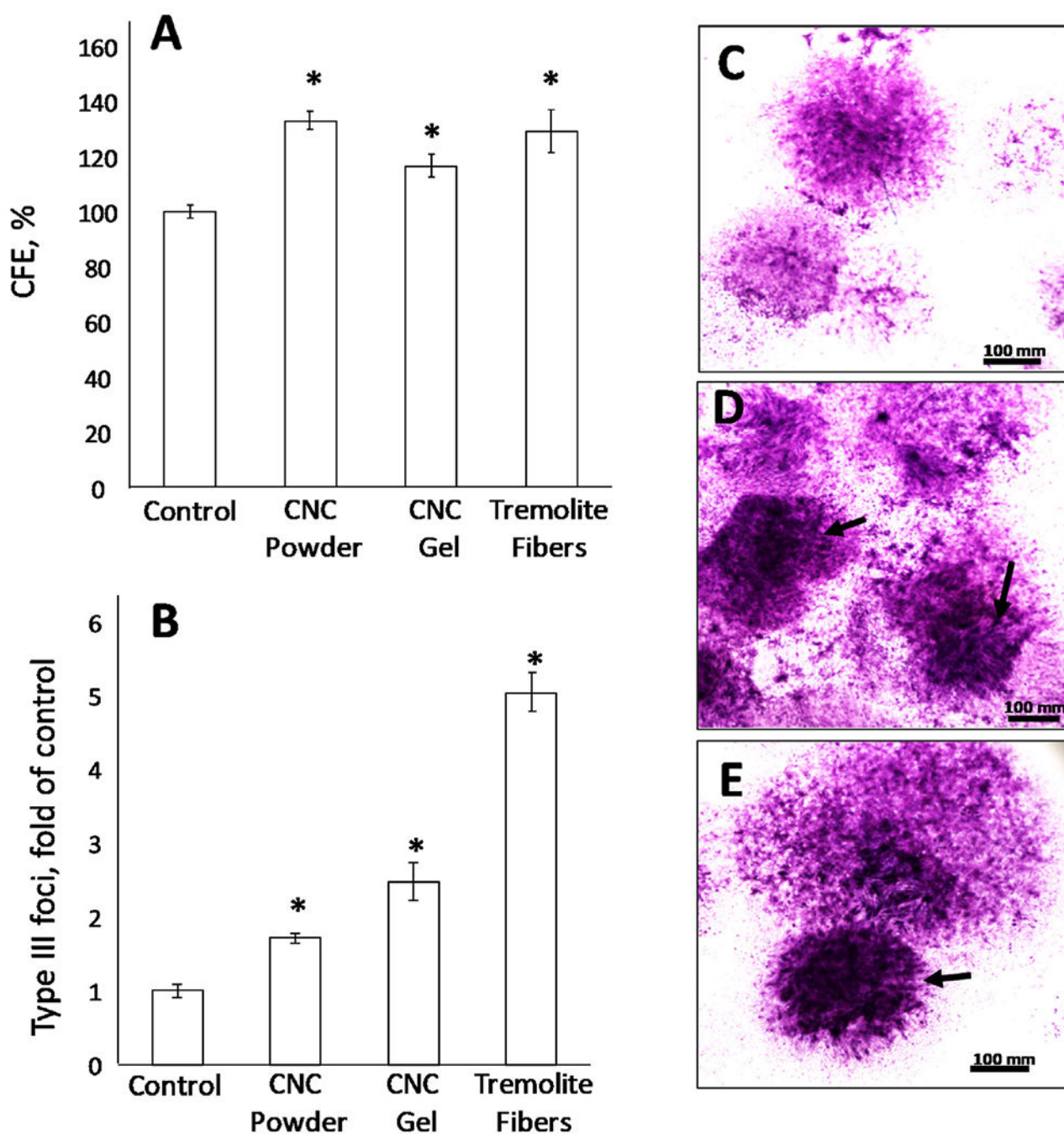
Fig. 2.
Altered morphological transformation in BEAS-2B cells exposed (4 weeks) to CNC
(powder or gel) and TF. Colony forming efficiency assay (A) and cells transformation assay
(B) based on Type III foci counts were performed on cells survived long-term exposure to
CNC powder/gel (30 μg/cm^2) or tremolite fibers (2.5 μg/cm^2). Representative images of
BEAS-2B cells from control groups (C) demonstrated either type I or type II foci. Type III
foci (arrows) presented basophilic staining, multi-layered cell growth, random cells
orientation and invasive growth into monolayer after exposure to CNC powder (D) and CNC

gel (E). The results are expressed as the mean ± SEM (n = 3), *indicate significant differences from control cells (p 0.05).
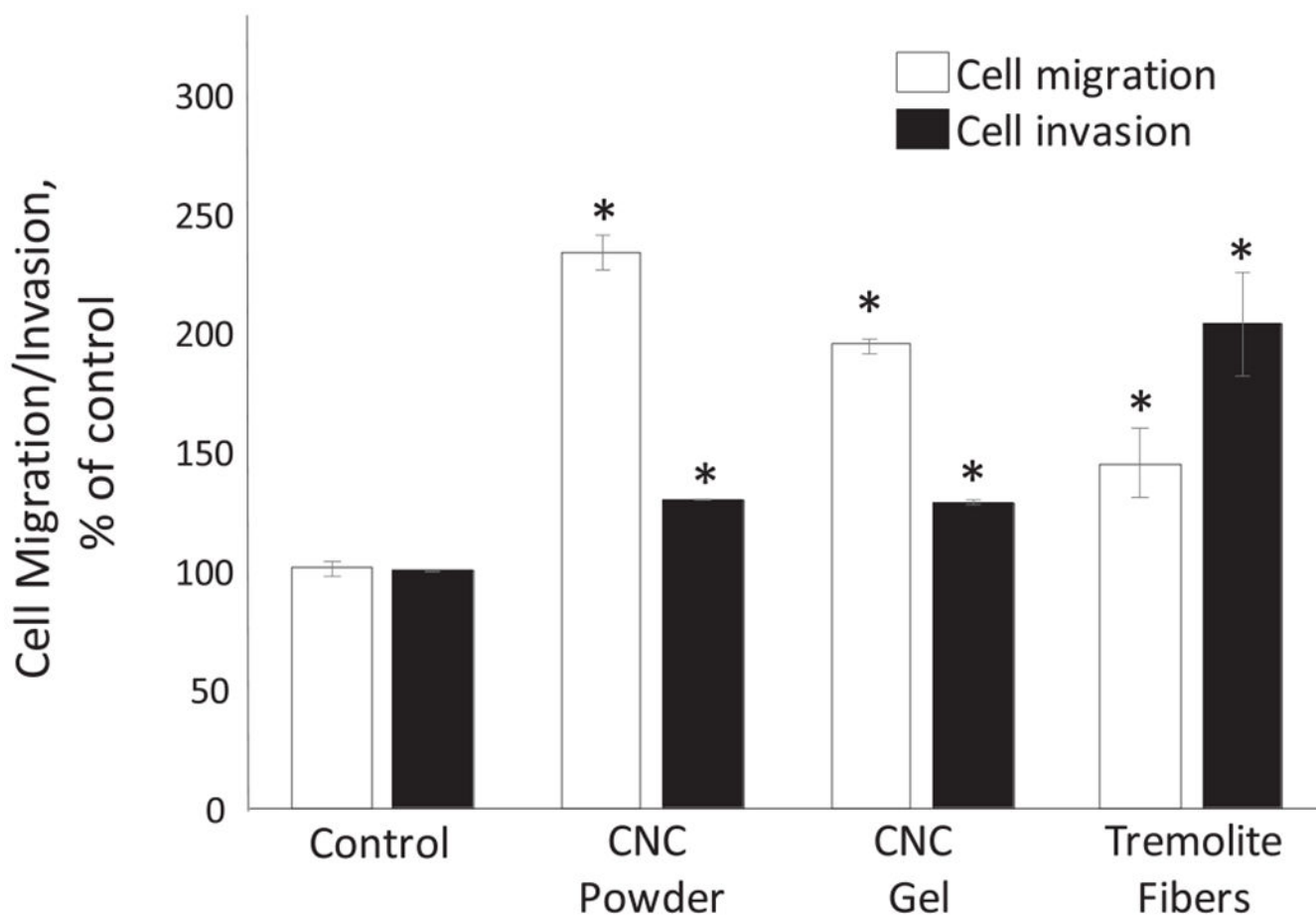
Fig. 3.

BEAS-2B cells migration and invasion was assessed after long-term exposure to cellulose nanomaterials and tremolite asbestos. Cells exposed to CNC (30 μg/cm^2) or tremolite respirable fibers (2.5 μg/cm^2) for 4 weeks (72 h/week) were seeded (1.5 × 10^5 cells) in an 8 μm pore size transwell chamber and incubated for 24 h. Migratory/invasive cells were stained on the bottom of the membrane prior to quantification at 560 nm. Open columns – correspond to cellular migration and black columns – represent cellular invasion. The results are expressed as the mean ± SEM (n = 3), *indicate significant differences from control cells (*p* 0.05).
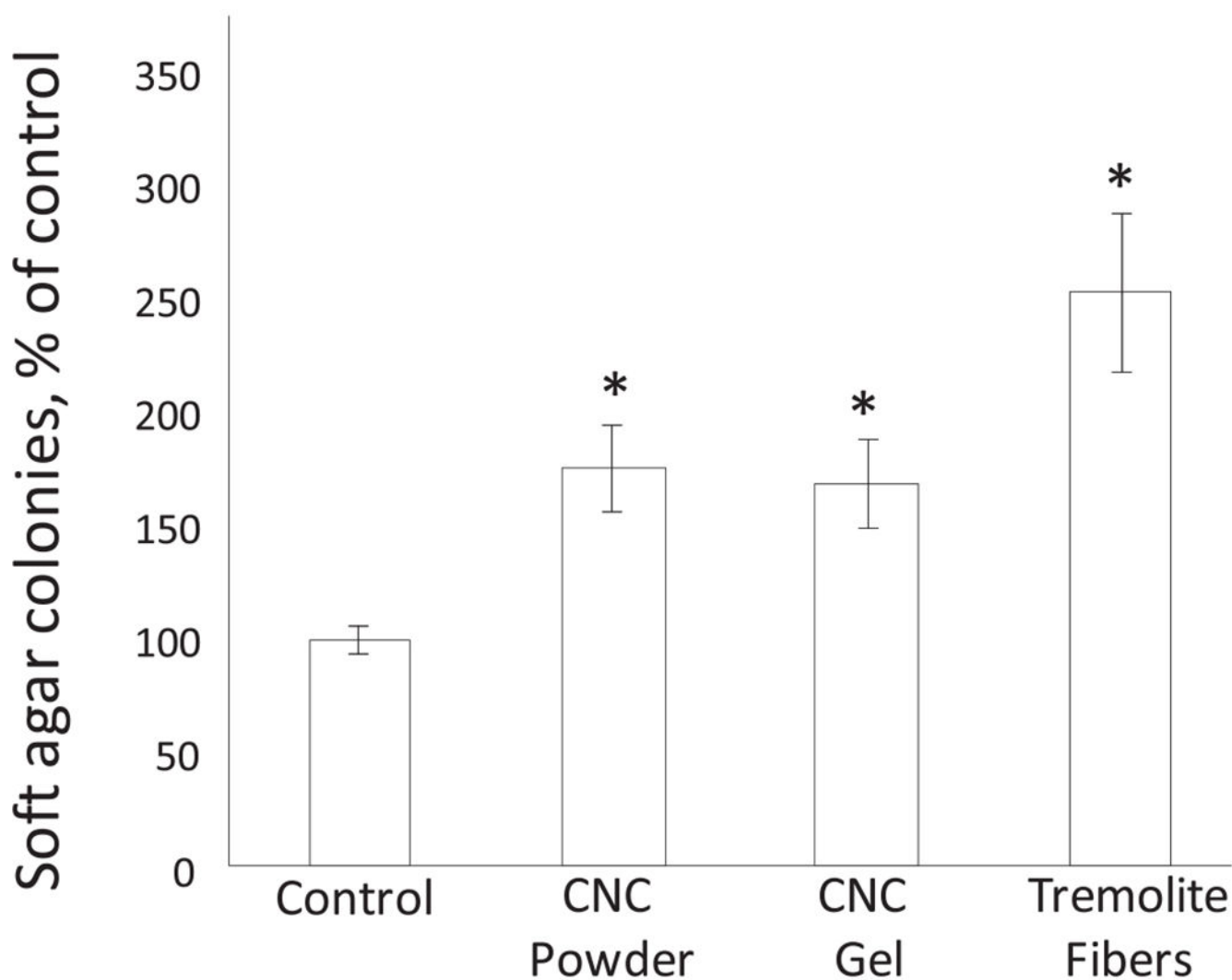
Fig. 4.
Anchorage-independent growth of human BEAS-2B cells exposed for 4 weeks to CNC materials (30 μg/cm^2) or tremolite fibers (2.5 μg/cm^2). Cells survived long-term exposure were seeded in 96 well plate (5×10^3 cells/well). Eight days later, colonies were stained and quantified at Ex/Em 485/520 nm. The results are expressed as the mean ± SEM (n = 3–6), * indicate significant differences from control cells (p 0.05).
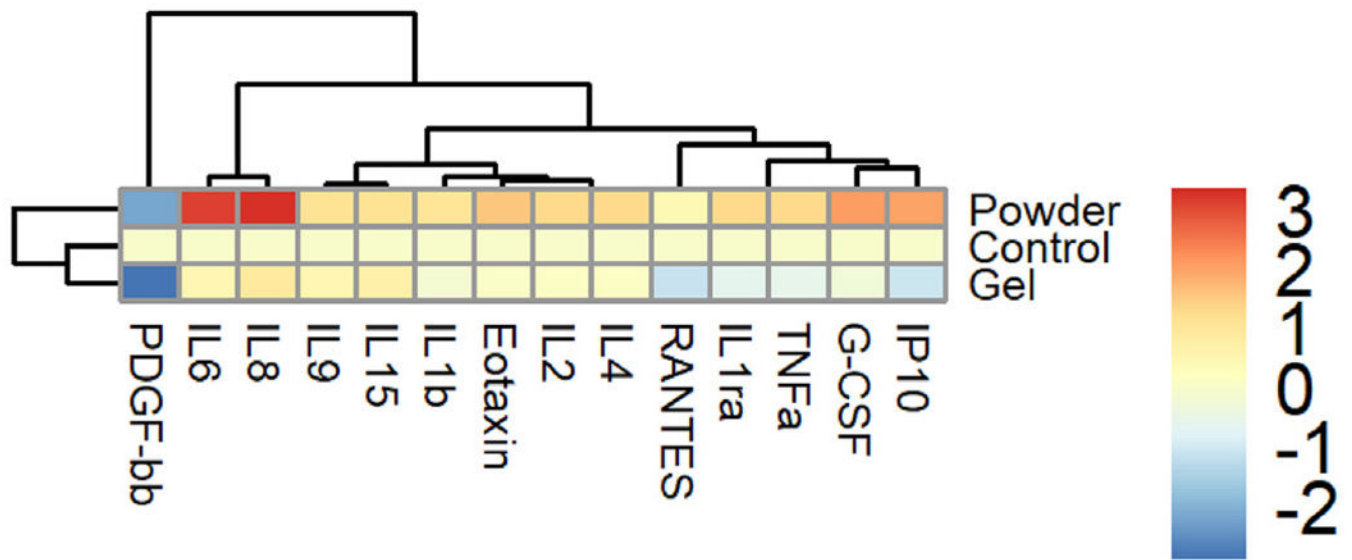
Fig. 5.
Analysis of differential cytokines/chemokines/growth factors responses in BEAS-2B cells upon long-term exposure (4 weeks) to CNC powder or gel. The two-way hierarchical clustering analysis of BEAS-2B control and exposed samples based on the inflammatory cytokines was performed using the Euclidean distance metric and ward.D2 distance linkage method. The dendrogram on the top clusters according to the cytokine profiles. The dendrogram on the left however indicated similarities in cytokines patterns among different CNC forms. The levels of various inflammatory factors investigated in this study are represented by shades of blue to red in the central heatmap, with highest values in dark red and the lowest in dark blue. A key showing the range of these values is also specified. (For interpretation of the references to color in this figure legend, the reader is referred to the Web version of this article.)